FTIR Analysis of Dimethyl Ether Decomposition Products Following Charge Transfer Ionization with Ar^+ under Matrix Isolation Conditions

Matthew G. K. Thompson and J. Mark Parnis*

Department of Chemistry, Trent University, Peterborough, Ontario, Canada, K9J 7B8

Received: July 28, 2008

Fourier transform infrared spectroscopic analysis has been performed on argon matrices formed following electron bombardment of argon/dimethyl ether mixtures. Products consistent with the ionization and subsequent fragmentation of dimethyl ether cation have been observed. Following ionization of dimethyl ether, fragmentation occurs that is consistent with ionization energy greater than 15 eV due to efficient charge transfer from dimethyl ether to Ar^+ as the major ionization process. Major products observed in the infrared spectra are methane, formaldehyde, $HCO^•$, CO, and Ar_2H^+. These products are consistent with the known fragmentation of photoionized dimethyl ether in a 15−16 eV ionization energy range. However, the observation of dehydrogenated products is consistent with additional abstraction of hydrogen from proximally located species isolated within the matrix. Analogous experiments employing CD_3OCH_3 give similar results, and the observed isotopically substituted products are consistent with the proposed fragmentation pathways.

Introduction

Previous studies in our research group have focused on the decomposition products of ions formed through electron bombardment of rare gas mixtures containing organic substrates, with the products isolated in the condensed rare gas.[1−3] The initially formed vibrationally hot ions can be stabilized under the relatively high pressures of the matrix isolation technique, thereby quenching higher-order decomposition processes and isolating the initial products following ion fragmentation. This technique therefore allows the verification of proposed decomposition pathways of ions formed in traditional mass spectrometry sources and provides complementary insights into the fragmentation chemistry of initially formed molecular ions. The decomposition of acetone under these conditions has provided extensive insight into several parallel and consecutive reaction pathways occurring following ionization of the acetone molecule.[3] The diverse chemistry observed through analysis of acetone, the simplest ketone species, has prompted our investigations in the chemistry of decomposition of other simple functional groups. Dimethyl ether (CH_3OCH_3) is the simplest molecule containing the ether functional group, and as a result, understanding the chemistry of this species is useful for building an understanding of the chemistry of larger homologous ether molecules. Additionally, the decomposition chemistry of cationic dimethyl ether has been well characterized by various ionization and mass spectrometric techniques[4−12] and with complementary theory investigating decomposition.[13−16] Comparison with such analyses allows us to further evaluate our electron bombardment matrix isolation infrared studies as a complementary technique to decomposition chemistry observed through mass spectrometric analysis.

Threshold photoelectron−photoion coincidence (TPEPICO) studies of CH_3OCH_3 have been conducted by Butler and co-workers,[7] and a complementary study of CD_3OCH_3 has been performed by Dutuit and co-workers.[8] Such studies reveal several insights into the different dissociation channels that can be accessed following ionization of dimethyl ether over a photoionization energy range covering 10−18 eV. In this range, the major primary decomposition pathways of ionized dimethyl ether are:

$$CH_3OCH_3 \rightarrow CH_3OCH_3^{•+}$$

$$AE = 10.02 \text{ eV}$$

$$CH_3OCH_3 \rightarrow CH_3OCH_3^{•+} \rightarrow CH_3OCH_2^+ + H^•$$

$$AE = 11.12 \text{ eV}$$

$$CH_3OCH_3 \rightarrow CH_3OCH_3^{•+} \rightarrow CH_3^• + H_2COH^+$$

$$AE = 11.75 \text{ eV}$$

$$CH_3OCH_3 \rightarrow CH_3OCH_3^{•+} \rightarrow HCO^+ + H_2 + CH_3^•$$

$$AE = 12.85 \text{ eV}$$

The $CH_3OCH_2^+$ species is the dominant primary fragmentation product at lower photoionization energies; however, several secondary dissociations of this species are observed following formation of the $CH_3OCH_2^+$ species with increasing internal energy. These major secondary processes can be summarized as:

$$CH_3OCH_3 \rightarrow CH_3OCH_2^+ + H^• \rightarrow HCO^+ + CH_4 + H^•$$

$$AE \geq 14.00 \text{ eV}$$

$$CH_3OCH_3 \rightarrow CH_3OCH_2^+ + H^• \rightarrow CH_3^+ + H_2CO + H^•$$

$$AE \geq 14.90 \text{ eV}$$

Isotope effects in the dissociation of CD_3OCH_3 have also been studied by TPEPICO by Dutuit and co-workers.[8] A summary of their results is in agreement with the results presented by Butler and co-workers[7] and gives the following primary isotopic dissociation processes for ionized CD_3OCH_3:

$$CD_3OCH_3 \rightarrow CD_3OCH_3^{•+} \rightarrow CD_3OCH_2^+ + H^•$$

$$AE = 10.95 \text{ eV}$$

* To whom correspondence should be addressed. E-mail: mparnis@trentu.ca (J. M. P.), mthompso@trentu.ca (M. G. K. T.).

10.1021/jp806689j CCC: $40.75
Published on Web 11/06/2008

$$CD_3OCH_3 \rightarrow CD_3OCH_3^{\bullet+} \rightarrow CD_2OCH_3^{+} + D^{\bullet}$$
$$AE = 11.04\ eV$$

$$CD_3OCH_3 \rightarrow CD_3OCH_3^{\bullet+} \rightarrow H_2COH^{+} + CD_3^{\bullet} \text{ or } D_2COD^{+} + CH_3^{\bullet}$$
$$AE = 11.75\ eV$$

$$CD_3OCH_3 \rightarrow CD_3OCH_3^{\bullet+} \rightarrow HCO^{+} + CD_3H + H^{\bullet}$$
$$AE = 11.97\ eV$$

$$CD_3OCH_3 \rightarrow CD_3OCH_3^{\bullet+} \rightarrow HCO^{+} + CD_3^{\bullet} + H_2$$
$$AE = 11.97\ eV$$

$$CD_3OCH_3 \rightarrow CD_3OCH_3^{\bullet+} \rightarrow DCO^{+} + CDH_3 + D^{\bullet}$$
$$AE = 11.97\ eV$$

$$CD_3OCH_3 \rightarrow CD_3OCH_3^{\bullet+} \rightarrow DCO^{+} + CH_3^{\bullet} + D_2$$
$$AE = 11.97\ eV$$

Again, higher internal energy in the resultant cation leads to products of secondary ion fragmentation:

$$CD_3OCH_3 \rightarrow CD_3OCH_2^{+} + H^{\bullet} \rightarrow CD_3^{+} + H_2CO + H^{\bullet}$$
$$AE > 14.9\ eV$$

$$CD_3OCH_3 \rightarrow CD_2OCH_3^{+} + D^{\bullet} \rightarrow CH_3^{+} + D_2CO + D^{\bullet}$$
$$AE > 14.9\ eV$$

Decomposition of ionized argon clusters containing a single dimethyl ether molecule has been previously reported by Stace.[17] In this work, the major method of ionization of dimethyl ether proposed in the larger argon clusters ($n > 12$) is charge transfer ionization by Ar_n^+ formed through electron ionization. Subsequently, charge is transferred from CH_3OCH_3 to Ar_n^+, yielding $Ar_n(CH_3OCH_3)^+$. By this ionization mechanism, ionized dimethyl ether has a maximum internal energy of 5.7 eV, and subsequent decomposition is explained on the basis of the relatively fast dissociation steps, compared with internal energy transfer to the argon cluster. Three major ions are observed, corresponding to the parent ion $Ar_n(CH_3OCH_3)^+$, and daughter ions, $Ar_n(CH_3OCH_2)^+$, and a particularly stable $Ar_n(CHO)^+$. The formation of their fragmentation products under gas-phase conditions is consistent with those proposed in studies of ionization and subsequent fragmentation of dimethyl ether,[5,7] and it is noted that the work is likely to share a common ground with matrix isolation studies such as those presented in this work.

Our investigations are in agreement with this supposition, and in this work, an analysis of the decomposition products of dimethyl ether following electron bombardment under argon-mediated matrix isolation conditions is presented. Our fragmentation products show excellent agreement with those previously observed for fragmentation from ionized dimethyl ether in the energy range of 15−16 eV. In the following sections, it can be seen that our results also demonstrate products consistent with additional reactivity of the initially formed species. This additional reactivity is likely due to neutralization of initially formed ions in the electron-rich environment of our matrix-isolation electron bombardment system and also due to re-encounter chemistry of initially formed products under the higher reaction pressures necessary for matrix isolation.

Experimental

The electron bombardment matrix isolation spectroscopy (EBMIS) apparatus used in these experiments has been described in detail in a previous publication.[3] Small modifications to the original design have been made, as described below. The general apparatus is comprised of an electron source and an ionization region. The gas mixture crosses the beam of electrons above the surface of a cold KBr spectroscopic window (15 K), where the reagents and fragments are collected for observation. A thoriated tungsten filament is used as a source of electrons, providing an electron beam focused over several centimeters by a 300 V potential difference between the electrode and a collecting pin near the surface of the spectroscopic window. The collector pin is parallel to the surface of the spectroscopic window to ensure that all gases entering the matrix have a maximum likelihood of undergoing ionization prior to isolation within the matrix. The collector pin also acts as a collector for the electrons allowing for measurement of the current of electrons with an ammeter during sample acquisition. Ionization current in these experiments was held between 10−20 μA for all experiments.

An MKS mass flow controller is used to direct dimethyl ether entrained in excess argon (typically 1:4000 CH_3OCH_3:argon ratios) into the ionization region. A small plastic tube is situated at the terminus of the gas-handling region, which promotes gases traveling directly through the focused beam of electrons, prior to condensation on the spectroscopic window. The temperature of the spectroscopic window is maintained near 15 K by an APD Displex closed-cycle helium refrigeration system. Following deposition of a matrix sample for a given experiment, the contents of the matrix are analyzed by FT-infrared absorption spectroscopy using a Bomem MB102 spectrometer, with the sample compartment modified to accommodate the matrix isolation assembly. Spectra are recorded in the 4000−400 cm^{-1} range of the IR, with a resolution of 1 cm^{-1}. Generally, 100 scans are coadded for a typical spectral acquisition. To minimize impurities and for maintaining low temperatures, the system is maintained under high vacuum conditions, with a nominal base pressure near 5×10^{-7} Torr.

Gas mixtures used in all experiments were prepared on an all-metal vacuum system, using standard manometric techniques. Dimethyl ether (99%, Sigma-Aldrich) and CD_3OCH_3 (>99% atom D, C/D/N Isotopes) were used directly from gas-cyclinders without additional purification. Research purity argon (Praxair, 99.995%) was used without further purification. In all experiments, the gas-flow rate was held constant at 1.00 standard cubic centimeter per minute (sccm), unless otherwise specified. A typical sample acquisition was 2 h, unless otherwise specified.

Results

A portion of an infrared difference spectrum of matrices formed from argon gas containing CH_3OCH_3 (1:4000 CH_3OCH_3:Ar) with and without electron bombardment is given as Figure 1. When no electron current is applied, all of the features in the spectrum correspond to absorptions of CH_3OCH_3 monomers isolated in argon,[18] or to small amounts of common matrix impurities such as H_2O, CO, or CO_2. When the infrared spectrum of a matrix formed following 300 V, 10−20 μA electron bombardment of the Ar/CH_3OCH_3 mixture is compared with that formed in the absence of electron bombardment, all of the infrared absorption features corresponding to CH_3OCH_3 isolated in argon are diminished. This observation is consistent with the destruction of dimethyl ether under electron bombardment conditions. Concurrently, many new features appear in the spectrum. A complete list of all new features observed under electron bombardment conditions is summarized below as Table 1. These features can be broken down into groups, with the

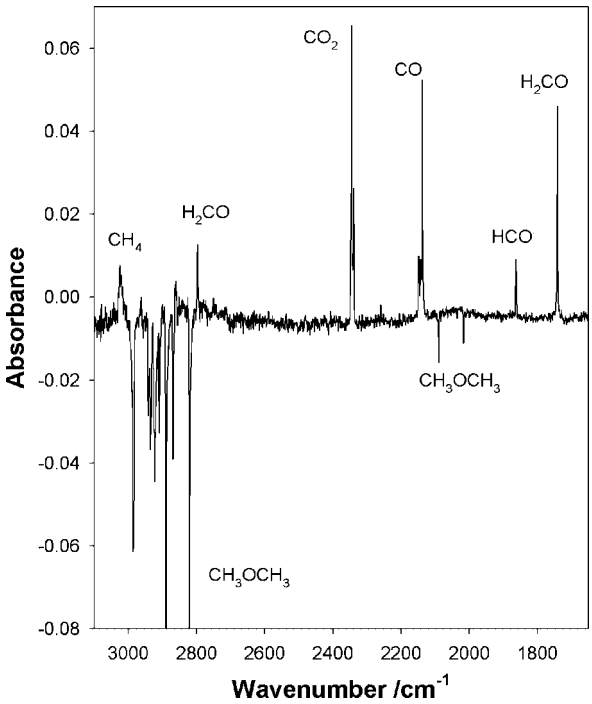

Figure 1. A portion of an infrared difference spectrum of a 1:4000 CH_3OCH_3:argon sample. Shown is a difference spectrum for the matrix formed under electron bombardment conditions from which the spectrum of a similar matrix formed with no electron bombardment is subtracted. Negative features correspond to dimethyl ether destruction, whereas positive absorbance features correspond to the labeled product.

major modes corresponding to the known infrared absorptions of argon-isolated formaldehyde, H_2CO (2797.0, 1741.5, 1498.0 cm^{-1}),[19] methane, CH_4 (3025.9, and 1304.8 cm^{-1}),[20] ketene, CH_2CO (2142.2, and 1115.0 cm^{-1}),[21] formyl radical, $HCO^{\bullet}$ (1862.7, and 1086.5 cm^{-1}),[22] carbon monoxide, CO (2148.4 (as a complex with H_2O), 2137.6 cm^{-1}),[20] and the proton-bound argon dimer cation, Ar_2H^+ (903.5 cm^{-1}).[23] Additionally, some changes in CO_2, and H_2O, the most common unavoidable matrix impurities, occur as a result of the electron bombardment technique. The only major feature that has not been assigned is an absorption that occurs at 1253.6 cm^{-1}. Otherwise, the remaining unassigned set of features at 1468, 1349, 1324, 1228, 1176, 1105, 944, 939, and 720 cm^{-1} are the weakest features in the spectrum and mostly likely result from one or more minor products of the reaction environment. These bands could be the result of further chemistry of the primary fragmentation products or due to complexes of primary decomposition products with matrix impurities. Alternatively, these may be modes due to CH_3OCH_2 radical, an expected product, though present in very low yields due to its unavoidable consumption via secondary decomposition pathways. Additional identification of these minor products would require further study.

As a means of investigating the mechanism of formation of formaldehyde and methane under the conditions of electron bombardment matrix isolation, a sample was prepared using 1:2000 CD_3OCH_3 in argon. The purpose was to investigate whether the formation of CH_4 involved a single CH_3OCH_3 or multiple CH_3OCH_3 molecules. In Figures 3 and 4, portions of the infrared spectra are presented as difference spectra for argon matrices formed from gas mixtures containing 1:2000 CD_3OCH_3: argon, without and with electron bombardment, as described above. When no electron bombardment is used, features corresponding to matrix-isolated CD_3OCH_3 are evident. As with the previous results, CO_2 and H_2O are also present as small matrix impurities. In the infrared spectra of matrices formed following 300 V, 10−20 μA electron bombardment of the gas mixture, a wealth of new features is observed. These features and their corresponding assignments are summarized for convenience in Table 1.

As above, the major new features can be broken into groups, and correspond to argon matrix-isolated formaldehyde, H_2CO (2797.2, 1741.7, 1498.1, and 1249.5 cm^{-1}),[19] d_2-formaldehyde, D_2CO (2178.4, 2069.0, 1696.6, and 987.2 cm^{-1}),[19] d_3-methane, CD_3H (3021.0, 2259.7, and 1287.2 cm^{-1}),[20] d_1-methane, CH_3D (1302.4, and 1155.5 cm^{-1}),[20] formyl radical, HCO (2480.5, 1862.3, and 1085.5 cm^{-1}),[22] d_1-formyl radical, DCO (1924.5, 1802.1, and 849.2 cm^{-1}),[22] carbon monoxide, CO (2148.6 (as a complex with H_2O), and 2137.1 cm^{-1}),[20] the proton-bound argon dimer cation, Ar_2H^+ (903.5 cm^{-1}),[23] and the deuteron-bound argon dimer cation, Ar_2D^+ (643.2 cm^{-1}).[23] No evidence for the pure isotopic methanes, CH_4 and CD_4 are observed, under these conditions. Also, little evidence for d_1-formaldehyde, HDCO, is observed. However, very weak bands at 2864.1, 2145.2, 1718.8, and 1029.6 cm^{-1} may be indicative of HDCO.[24] The lack of intensity associated with such bands within the observed infrared spectra suggests that isotopic mixing does not extensively occur in these experiments. These results are consistent with a dominant mechanism that involves the decomposition of a single dimethyl ether molecule to yield corresponding products, as discussed below.

The only major feature that cannot be assigned in the CD_3OCH_3-containing experiments is the absorption at 999.6 cm^{-1}. Otherwise, the remaining unassigned set of features at 2221, 2117, 2112, 2023, 2019, 1729, 878, 559, 508, and 492 cm^{-1} are the weakest features in the spectrum and are most likely associated with one or more minor products of the reaction environment. As before, these products could result from further chemistry of the primary fragmentation products or possibly as complexes of primary decomposition products with matrix impurities. Alternatively, these may be the deuterated counterparts of the expected CD_3OCH_2/CD_2OCH_3 radicals. In either case, the features are likely deuterium containing counterparts of the unassigned features listed when CH_3OCH_3 is used. Additional identification of these very minor products would require further study.

Discussion

It seems clear based on the infrared spectra presented in Figures 1 and 2 that electron bombardment of gas mixtures containing dilute CH_3OCH_3 in argon results in significant fragmentation of the dimethyl ether species. On the basis of the work of Butler et al.[7] and of Dutuit and co-workers,[8] the expected fragments in the current matrix-isolation FTIR absorption experiments would be neutral, radical, and/or ionic forms of: CH_3OCH_2, CH_3, CH_4, H_2COH, H_2CO, HCO, H_2, and H. Similarly, when CD_3OCH_3 is used, the expected products would be neutral, radical and ionic forms of: CD_3OCH_2, CD_2OCH_3, H_2COH, D_2COD, CD_3, CH_3, HCO, DCO, CD_3H, CH_3D, H_2, D_2, H, and D. However, in the results of the current study under matrix isolation conditions using FTIR analysis, the major observed products observed through their absorption bands in the infrared spectra of matrices formed following electron bombardment of Ar/CH_3OCH_3 mixtures are CH_4, H_2CO, $HCO^{\bullet}$, CO, and Ar_2H^+. Additionally, when matrices are formed following electron bombardment of similar Ar/CD_3OCH_3 mixtures, the major products observed through the infrared absorption spectrum are: H_2CO, D_2CO, CD_3H, CH_3D, $HCO^{\bullet}$,

TABLE 1: Infrared Absorption Positions of Products Formed via Electron Bombardment of Dimethyl Ether Isotopomers in Argon

CH_3OCH_3 in argon with electron bombardment				CD_3OCH_3 in argon with electron bombardment			
wavenumber	species[a]	wavenumber	species[a]	wavenumber	species[a]	wavenumber	species[a]
3025.9	CH_4	1498.0	H_2CO			1498.1	H_2CO
		1349.1		3021.0	CD_3H		
		1324.3		2864.1	HDCO?		
2797.0	H_2CO	1304.8	CH_4	2797.2	H_2CO		
2480.5	HCO					1302.4	CDH_3
2345.1	CO_2			2343.7	CO_2	1287.2	CD_3H
2338.5	CO_2	1253.6		2338.3	CO_2		
				2259.7	CD_3H	1249.5	H_2CO
		1228.0		2220.6			
		1176.0		2178.4	D_2CO		
				2148.6	CO	1155.5	CDH_3
2148.4	CO	1115.0	ketene?	2145.2	HDCO?		
2142.2	ketene?	1105.0					
2137.6	CO	1086.5	HCO	2137.1	CO	1085.5	HCO
				2132.0		1029.6	HDCO?
				2117.0		999.6	
				2111.6		987.2	D_2CO
		944.0		2069.0	D_2CO		
		939.0		2023.0			
		903.5	Ar_2H^+	2019.1		903.5	Ar_2H^+
				1924.5	DCO	877.5	
1862.7	HCO			1862.3	HCO	849.2	DCO
		720.7		1802.1	DCO		
1741.5	H_2CO	663.0	CO_2	1741.7	H_2CO	663.0	CO_2
		662.0	CO_2	1728.8		661.6	CO_2
				1718.8	HDCO?	643.2	Ar_2D^+
				1696.6	D_2CO	558.5	
1624.3	H_2O			1623.3	H_2O	508.4	
1608.3	H_2O			1607.6	H_2O	492.4	

[a] Product assignments labeled followed by "?" indicate a tentative product assignment.

$DCO^{\bullet}$, CO, Ar_2H^+, and Ar_2D^+. No absorptions due to the methyl radical or any of its isotopomers are observed in any of our spectra. Furthermore, none of the previously listed ion decomposition reactions, which represent the expected fragmentations, yield CO as a final product. Therefore, additional factors must be present in our work that can explain the absence of CH_3 radical, the appearance of CO, and the formation of the proton/deuteron-bound argon dimers.

In the related results of Stace,[17] large argon clusters ($n > 12$) containing dimethyl ether were ionized by electron impact, and charge transfer from the ionized argon cluster to dimethyl ether was proposed as the dominant ether ionization pathway, given the excess of argon present. The major products observed in the mass spectra of Stace were $Ar_n(CH_3OCH_3^+)$, $Ar_n(CH_3OCH_2^+)$, and $Ar_n(HCO^+)$. The current matrix-isolation work has a great excess of argon, which we believe is comparable to the conditions employed for larger Ar_n clusters in the related work of Stace. Therefore, the most likely ionized species in the reaction environment is indeed argon, and we believe that the major ionization mechanism of dimethyl ether under our conditions results from the following processes:

$$Ar + e^- \rightarrow Ar^{\bullet+} + 2\,e^-$$

$$Ar^{\bullet+} + CH_3OCH_3 \rightarrow Ar + CH_3OCH_3^{\bullet+}$$

The resultant dimethyl ether cation (used as the starting species in Schemes 1−3 below) is thus formed with excess internal energy.

The maximum internal energy of the dimethyl ether cation formed via this process can be obtained by evaluating IP(Ar) − IP(CH_3OCH_3) = 15.8 − 10.0 = 5.8 eV. This internal energy can then be available for subsequent ion decomposition. Therefore, any ionic fragmentation process with an appearance energy up to 15.8 eV may be possible following dimethyl possible ether charge transfer to $Ar^{\bullet+}$, dependent on the fraction of the charge transfer energy that is conserved in the dimethyl ether cation following electron transfer. Such an energy value is a useful boundary when considering the possible pathways accounting for fragmentation in our apparatus. According to the reaction equations listed in the above discussion, this should allow any of the fragmentation pathways with photoionization appearance energy in the range of 10−15.8 eV to be viable processes. However, many of the processes yield similar products, and therefore some additional analysis of the energetics is required to rationalize completely the products observed in the current matrix work.

The relative ion yields following photoionization over the range of 10–18 eV are presented in the results of Butler et al.,[7] in the form of a breakdown curve of the dimethyl ether cation. In the range of 10−11 eV, only dimethyl ether cations are formed following photoionization of the parent molecule. Near 11.0 eV, the [parent-H]$^+$ (i.e., $CH_3OCH_2^+$) is formed as the dominant ion. The yield of the [parent-H]$^+$ slowly decreases as the ionization energy is increased to 12 eV, due to production of H_2COH^+ in small yields via a competitive process branching directly from the parent dimethyl ether cation. This formation of the H_2COH^+ (and the neutral fragment $CH_3^{\bullet}$) occurs as a consistent, albeit minor, process over the 12−16 eV range, with maximum production near 14.5 eV. Moreover, the [parent-H]$^+$ species decays slowly up to 14 eV, at which point drastic decay occurs between 14 and 15 eV, and virtually no $CH_3OCH_2^+$ is present by ionization energy of 15.5 eV. The loss of the [parent-H]$^+$ species in this region is due to the subsequent dissociation

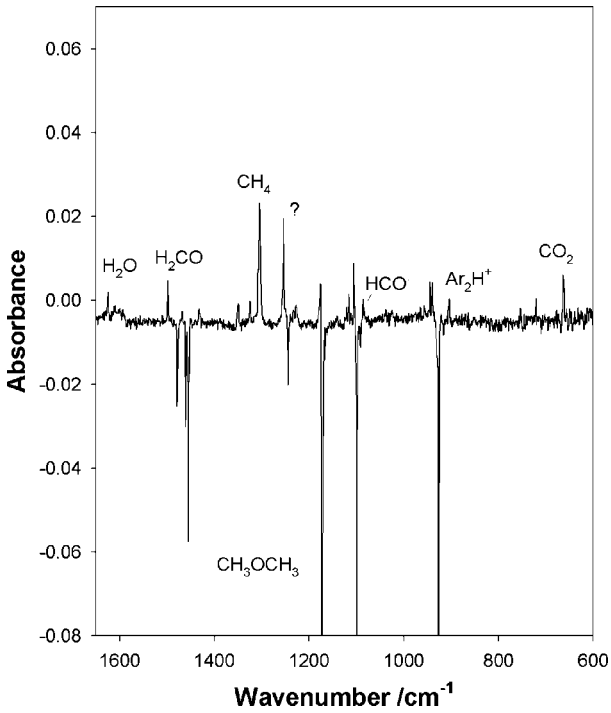

Figure 2. A portion of an infrared difference spectrum of a 1:4000 CH_3OCH_3:argon sample. Shown is a difference spectrum for the matrix formed under electron bombardment conditions from which the spectrum of a similar matrix formed with no electron bombardment is subtracted. Negative features correspond to dimethyl ether destruction, whereas positive absorbance features correspond to the labeled product. The feature marked ? is an unidentified product of the reaction environment.

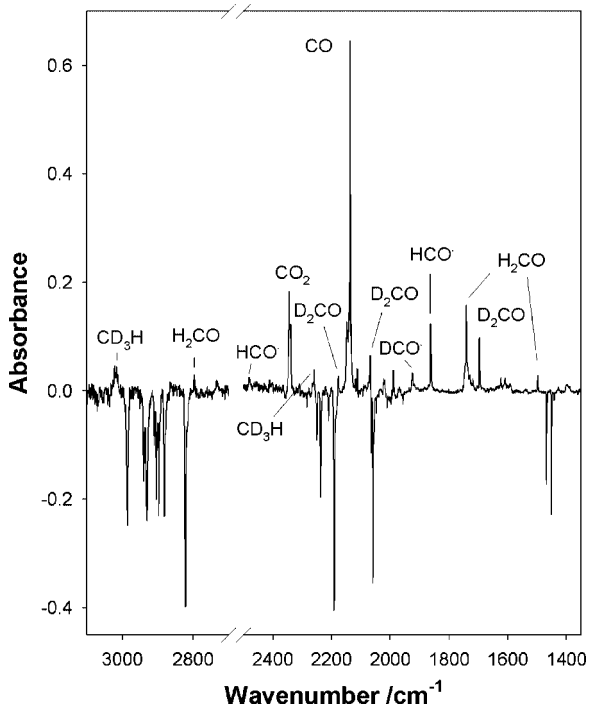

Figure 3. Portions of an infrared difference spectrum of a 1:2000 CD_3OCH_3:argon sample. Shown is a difference spectrum for the matrix formed under electron bombardment conditions from which the spectrum of a similar matrix formed with no electron bombardment is subtracted. Negative features correspond to CD_3OCH_3 destruction, whereas positive absorbance features correspond to the labeled product.

of energized $CH_3OCH_2^+$ to yield HCO^+ (and either of [$CH_3^\bullet$ and H_2] or [CH_4 and $H^\bullet$] as neutral fragments) between 14 and

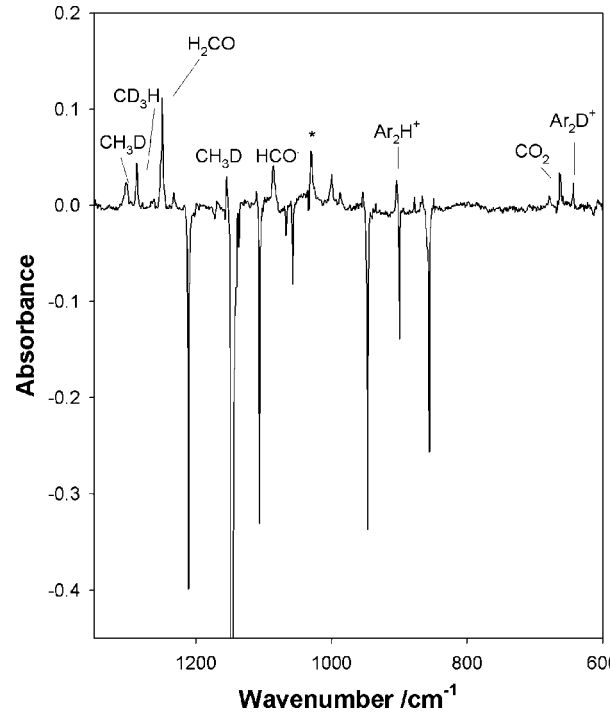

Figure 4. A portion of an infrared difference spectrum of a 1:2000 CD_3OCH_3:argon sample. Shown is a difference spectrum for the matrix formed under electron bombardment conditions from which the spectrum of a similar matrix formed with no electron bombardment is subtracted. Negative features correspond to CD_3OCH_3 destruction, whereas positive absorbance features correspond to the labeled product. The feature marked with * is an unidentified product of the reaction environment.

14.9 eV. Finally, more energetic $CH_3OCH_2^+$ yields the onset of CH_3^+ (and the neutral fragments H_2CO and $H^\bullet$) beyond 15 eV, accounting for the additional loss of the [parent-H]$^+$ observed in this region of the breakdown curve.

It is worth noting that, in the photoionization region of 12−14 eV, greater than 80% of the relative abundance of ions formed are the [parent-H]$^+$ species, at the exclusion of other products save a minor amount of H_2COH^+ and the corresponding neutral fragment $CH_3^\bullet$. The infrared absorption spectra of the matrices formed in this work contain products other than those expected in this region. It therefore seems unlikely that the dimethyl ether cation formed under electron bombardment matrix isolation conditions is formed with internal energy corresponding to photoionization in the 12−14 eV range. Charge transfer from $Ar^{\bullet+}$ can give a maximum of 15.8 eV, whereas the IP of dimethyl ether is 10.02 eV;[7,8] therefore the formation of dimethyl ether with internal energy of 5 eV is not unexpected. Additionally, because the neutral argon atom formed has no rotational or vibrational modes in which to retain internal energy, any energy the species retains during electron transfer would need to be translational energy. A significant acceleration of the heavy neutral argon following electron transfer is unlikely, suggesting that following the electron transfer, the majority of the internal energy is conserved within CH_3OCH_3. Therefore, it is most likely that the dimethyl ether cation is formed in the 15−15.8 eV apperance energy range. In this region of the breakdown curve of Butler,[7] almost no [parent-H]$^+$ is observed, as the energized ion dissociates via secondary channels to form both HCO^+ (and corresponding neutrals) and competitively CH_3^+ (and corresponding neutrals). The absence of the [parent-H] species supports the

SCHEME 1: First Fragmentation Mechanism Proposed for Dimethyl Ether Ionized under Conditions of Electron Bombardment Argon Matrix Isolation Conditions

Step 1 – gas	$CH_3OCH_3^{\bullet+*} \rightarrow H_2COH^+ + CH_3^\bullet$	Dissociation
Step 2 – hp	$\{H_2COH^+ + CH_3^\bullet\} + e^- \rightarrow \{H_2COH^\bullet + CH_3^\bullet\}$	Neutralization
Step 3 – hp	$\{H_2COH^\bullet + CH_3^\bullet\} \rightarrow H_2CO + CH_4$	Abstraction by $CH_3^\bullet$
Step 3b – hp	$\{H_2COH^\bullet + CH_3^\bullet\} \rightarrow\rightarrow CO + CH_4 + H_2$	CO formation

SCHEME 2: Second Competitive Fragmentation Mechanism Proposed for Ionized Dimethyl Ether under Conditions of Electron Bombardment Matrix Isolation

Step 1 – gas	$CH_3OCH_3^{\bullet-} * \rightarrow CH_3OCH_2^+ + H^\bullet \rightarrow HCO^+ + CH_4 + H^\bullet$	Fragmentation
Step 2 – hp	$HCO^+ + e^- \rightarrow HCO^\bullet *$	Electron capture
Step 3 – hp	$HCO^\bullet * \rightarrow CO + H^\bullet$	Dissociation

SCHEME 3: Third Competitive Fragmentation Mechanism Proposed for Dimethyl Ether Ionized under Conditions of Electron Bombardment Matrix Isolation

Step 1 – gas	$CH_3OCH_3^{\bullet+} \rightarrow CH_3^- + H_2CO + H^\bullet$	Fragmentation
Step 2 – hp	$\{CH_3^+ + H_2CO\} + e^- \rightarrow \{CH_3^\bullet * + H_2CO\}$	Electron capture
Step 3 – hp	$\{CH_3^\bullet * + H_2CO\} \rightarrow CH_4 + HCO^\bullet$	$H^\bullet$ abstraction

notion that the initially formed ion following electron bombardment under matrix isolation conditions has internal energy corresponding to that of dimethyl ether cation formed via photionization in the 15−15.8 eV range. This is further supported by the observation of absorption bands due to higher-order fragments of the dimethyl ether cation within the matrix infrared absorption spectra. Therefore, assuming this energy boundary, according to the ions present in the breakdown curves of Butler et al. near AE = 15.8 eV,[7] the expected products isolated in the matrix would result from the following reactions:

$$CH_3OCH_3 \rightarrow CH_3OCH_3^{\bullet+} \rightarrow H_2COH^+ + CH_3^\bullet \qquad AE > 11.75\ eV \quad (1)$$

$$CH_3OCH_3 \rightarrow CH_3OCH_2^+ + H^\bullet \rightarrow HCO^+ + CH_4 + H^\bullet \qquad AE \geq 14.00\ eV \quad (2a)$$

$$\text{Or } CH_3OCH_3 \rightarrow CH_3OCH_2^+ + H^\bullet \rightarrow HCO^+ + H_2 + CH_3^\bullet \qquad AE \geq 14.00\ eV \quad (2b)$$

$$CH_3OCH_3 \rightarrow CH_3OCH_2^+ + H^\bullet \rightarrow CH_3^+ + H_2CO + H^\bullet \qquad AE \geq 14.90\ eV \quad (3)$$

Indeed, CH_4 and H_2CO are observed as major products through analysis of the infrared spectra in the current matrix isolation results. However, none of the listed cations or radicals in the above reactions are observed in our IR spectra. It is worth noting that the matrix isolation experiments are performed at much higher pressures than the corresponding TPEPICO results, and therefore ion−molecule re-encounter chemistry is likely. Furthermore, the electron bombardment matrix isolation technique involves scattered secondary electrons, which can be scavenged during matrix formation by cations formed in the primary processes. Therefore, significant chemistry due to ion neutralization can also occur. In the context of these ideas, the steps outlined in Schemes 1–3 are proposed as a means of reconciling the expected gas-phase results with those observed within the matrix isolation experiments, following dimethyl ether cation formation.

In reaction (1) above, both H_2COH^+ and $CH_3^\bullet$ are expected products. However, neither of these two species is observed in the matrix infrared spectra. During matrix condensation, the relatively high pressures necessary for argon matrix formation would inhibit the migration of these two species following fragmentation of the parent ion. Therefore, when these species are formed under the conditions of matrix isolation, it is very likely that they reside in close proximity. The presence of significant scattered secondary electrons allows protonated formaldehyde species to become neutralized. This would produce $H_2COH^\bullet$ near $CH_3^\bullet$. The close proximity of these two radical species would allow $H^\bullet$ abstraction by $CH_3^\bullet$ yielding CH_4 and H_2CO. This step also eliminates $CH_3^\bullet$, a species that is not observed in any of the current infrared spectra. Additionally, elimination of H_2 following electron capture by H_2COH^+ (analogous to that proposed by Burgers and Holmes)[25] may give rise to HCO radical near $CH_3^\bullet$, ultimately leading to formation of CO and CH_4. Each of CH_4, H_2CO, and CO are observed in the infrared absorption spectra of the matrix isolation experiments. Thus, the above steps represent a plausible explanation accounting for the observation of these two species, which is consistent with all sets of results.

When the isotopomeric CD_3OCH_3 is used, both H_2COH^+ with $CD_3^\bullet$ and D_2COD^+ with CH_3^+ would be expected in the matrix. The proposed neutralization and H/D transfer steps would then yield CD_3H with H_2CO or CDH_3 with D_2CO respectively but would not yield any mixed isotopes of formaldehyde or the pure isotopic methanes. When CD_3OCH_3 is subjected to electron bombardment matrix isolation conditions, CD_3H, H_2CO, CDH_3, and D_2CO are indeed observed in the corresponding IR spectra as major products. This result provides further support for the proposed neutralization and $H^\bullet/D^\bullet$ steps under the conditions of electron bombardment matrix isolation. Therefore, Scheme 1 is proposed as a means of reconciling the gas-phase results with the higher pressure, electron rich (indicated with hp) conditions of the electron bombardment matrix isolation technique.

In the competitive reaction (2a) or (2b) above, the expected products isolated in the matrix would be either a) CH_4, $H^\bullet$, HCO^+ or b) $CH_3^\bullet$, H_2, and HCO^+. Both (2a) and (2b) have similar thermochemical onset values, and thus the specific product formation channel was not previously distinguishable. The two reactions (2a) and (2b) do have one infrared active species, which could be used to distinguish the two mechanistic

steps, specifically the formation of CH_4 versus $CH_3^\bullet$. Again, no evidence is present in any of our infrared spectra for the formation of $CH_3^\bullet$, whereas CH_4 is present under all conditions as a major product when CH_3OCH_3 is used. Therefore, we believe that of the two reaction pathways, reaction (2a) is the reaction pathway leading to products under our conditions.

In keeping with this reasoning, reaction (2a) leads to the formation of HCO^+ as a major product, although no evidence is present in the infrared absorption spectra of our matrices for HCO^+. Similar to the argument proposed for H_2COH^+ above, it is likely that this species can capture an electron in the electron-rich environment during matrix condensation, forming $HCO^\bullet$. However, the formation of this species by electron capture is exoergic by 9.8 eV. Thus, this species may dissociate along the H−C bond following electron capture, yielding $H^\bullet$ and CO.[26] This proposed step could then explain the observation of CO as a major product in the matrix infrared spectra.

Correspondingly, when CD_3OCH_3 is used, reaction (2a) would predict that $H^\bullet$, $D^\bullet$, CD_3H, CH_3D, HCO^+, and DCO^+ would be produced. CD_3H and CH_3D are observed in the infrared spectrum following electron bombardment and subsequent matrix formation. Additionally, the proposed electron capture steps leading to $HCO^\bullet/DCO^\bullet$ dissociation would yield CO along with $H^\bullet/D^\bullet$. The products observed when CD_3OCH_3 is used are consistent with the proposed steps, and therefore it seems likely that such steps are occurring within the matrix environment. Therefore, Scheme 2 is presented to summarize the reconciliation of the gas-phase steps with the higher-pressure, electron-rich matrix isolation conditions (indicated by hp).

Finally, in the third competitive reaction (3), CH_3^+ is formed along with H_2CO and $H^\bullet$. Within the matrix environment, the CH_3^+ species could be expected to neutralize yielding $CH_3^\bullet$ in close proximity to H_2CO, as predicted for other cationic species. However, no evidence for methyl radical is observed under any of our reaction conditions. It might be expected that hydrogen atom abstraction from H_2CO by methyl radical would be relatively easy. Thermodynamically, the new C−H bond of methane would be more favorable than the C−H bond of formaldehyde, thereby demonstrating a thermochemically viable process. Although this reaction does have an energy barrier,[27] the process is likely facilitated by the energy released during electron capture of the CH_3^+ species. The resultant species would be CH_4 and $HCO^\bullet$, both of which are observed in the infrared spectra of the formed matrices. Additionally, such a step regenerates $HCO^\bullet$, a major product in the infrared spectra. This species should be destroyed following dissociative electron capture, and therefore, the hydrogen abstraction by methyl radical accounts for a low-energy formation pathway of $HCO^\bullet$, while simultaneously eliminating the unobserved $CH_3^\bullet$.

When CD_3OCH_3 is used, both CH_3^+ alongside D_2CO and CD_3^+ alongside H_2CO would be expected. In the proposed steps, neutralization of the cationic methyl isotopomer and D/H abstraction would yield CDH_3 and $HCO^\bullet$, as well as CD_3H and $DCO^\bullet$. All of these species are observed in the infrared spectra when CD_3OCH_3 is used, and thus this provides additional support for the proposed steps. Therefore, Scheme 3 is presented to summarize the reconciliation of the gas-phase steps with the higher-pressure, electron-rich matrix isolation steps (indicated by hp).

It is worth noting that, in steps where the very light $H^\bullet$ or $D^\bullet$ are generated, the resultant atom is likely generated with significant translational energy. As well, this atom is known to diffuse quite readily within the argon lattice of the matrix,[28] decreasingly the probability of any radical-$H^\bullet$ recombination with the other fragments formed in the process that originated the hydrogen atom.

All of the products in the terminating steps of Schemes 1, 2, and 3 are observed in the current infrared results, following ionization and decomposition of CD_3OCH_3, with no step generating an unobserved product. Additionally, all of the steps are supported by TPEPICO measurements reported previously.[7,8] Additionally, no significant isotopic scrambling is observed in the formaldehyde species generated, as was noted in the work of Dutuit.[8] Therefore, we believe that the schemes presented above account for the dominant products observed in our work and that the major processes are most consistent with dimethyl ether internal energies in the 5−6 eV range. By these mechanistic steps, only the presence of Ar_2H^+ and Ar_2D^+ has not been addressed, and therefore the formation of this species in the matrix isolation experiments requires additional consideration.

Formation of Ar_2H^+/Ar_2D^+. The presence of modes associated with Ar_2H^+ in the infrared spectrum[23] following electron bombardment of dimethyl ether was originally believed to result from proton transfer from ionized water impurities during electron bombardment matrix isolation. However, the formation of Ar_2D^+ when CD_3OCH_3 is used, implicates the dimethyl ether molecule as the origin of the H/D nucleus. The schemes and energetics presented above imply that significant $H^\bullet/D^\bullet$ will be present in our matrices following dimethyl ether fragmentation to yield the primary products observed in the infrared spectra. Additionally, these atomic H/D are formed in the gas phase, during the initial ionization. It is quite likely that the light H/D atoms leave the initial dissociation with significant translational energy, making them quite mobile under matrix isolation conditions. Therefore, once formed, the H/D atoms would be expected to be homogeneously distributed through the system, much as the argon hosts, during the electron bombardment process.

The ionization potential of a hydrogen atom is approximately 13.6 eV, whereas that of an argon atom is 15.8 eV. Therefore, charge transfer ionization from H/D to Ar^+ is a viable reaction whenever both species are present. As a result, when H/D atoms are present during ionization, these would represent a charge sink, resulting in formation of H^+/D^+. The presence of H^+/D^+ in close proximity to argon could form ArH^+ or ArD^+, which when isolated in the matrix would become Ar_2H^+ or Ar_2D^+, as observed. Such a species should be expected to neutralize, similar to other cation species expected in the matrix. However, if a corresponding counterion were present, such a neutralization may be inhibited. In any event, the formation of Ar_2H^+/Ar_2D^+ by charge transfer ionization of $H^\bullet/D^\bullet$ seems like the most likely mechanism in these experiments. Therefore, the observation of Ar_2H^+/Ar_2D^+ may serve as an indirect sensor for the presence of $H^\bullet/D^\bullet$ when they are present in the electron bombardment matrix isolation apparatus.

Formation of HDCO. In the above schemes, the formation of methane and formaldehyde appear as major reaction products under matrix isolation conditions, following fragmentation of ionized dimethyl ether. When CD_3OCH_3 is used, the major products are H_2CO and CD_3H as well as D_2CO and CH_3D, whereas no signature of CH_4 or CD_4 is observed. There are, however, some modes that may be due to the formation of HDCO in the argon matrix. The schemes proposed for product formation above do not allow for intramolecular isotopic mixing, as they are isotopically selective for the products that are formed. It is worth noting that, in the schemes above, the only radical product species expected to be isolated in the matrix are $HCO^\bullet/DCO^\bullet$. Additionally, the schemes suggest that $H^\bullet/D^\bullet$ atoms are

able to migrate throughout the matrix during condensation, which is supported through Ar_2H^+/Ar_2D^+ formation. It would not, therefore, be unreasonable to expect that $HCO^{\bullet}/DCO^{\bullet}$ radicals could encounter respective $D^{\bullet}/H^{\bullet}$ atoms during condensation, thereby forming HDCO by radical−radical recombination. This would yield HDCO, or the pure isotopic H_2CO/D_2CO (already major products).

That HDCO could be formed by radical−radical recombination suggests that the same mechanism should be true for $CH_3^{\bullet}/CD_3^{\bullet}$ formed within the matrix as well. However, as discussed above, the H/D abstraction steps eliminating methyl radicals are likely quite fast, even under the conditions of matrix isolation. Thus, the lifetime of methyl radicals within the matrix environment is likely too short to encounter free H/D atoms under the current reaction conditions. The fast hydrogen atom abstraction by methyl radicals yields the very HCO implicated in HDCO formation, and therefore the previous observation of HCO radical scavenging H/D is more consistent with the current available data. This proposal would thus account for all of the major products observed in the corresponding infrared spectra.

Unidentified Infrared Spectral Features. The presence of two key features at 1253 cm^{-1} (CH_3OCH_3) and 999 cm^{-1} (CD_3OCH_3) as unassigned features remains a mystery. These features, along with other minor features listed in the results, may be attributed to the $CH_3OCH_2^{\bullet}$, as this species should be present under the conditions employed here. However, if the internal energy of the initially formed dimethyl ether cation is near 5 eV, the yield of $CH_3OCH_2^{\bullet}$ should be quite small. Nevertheless, some of this species could be stabilized by repeated third body collision with argon, as a result of the matrix isolation technique. Thus, the feature at 1253 cm^{-1} may result from this species, and thus the species at 999 cm^{-1} may represent an isotopomer of the same species. Given that this is the most likely species expected in this work, we tentatively assign these features as isotopomers of $CH_3OCH_2^{\bullet}$; however, more work will be required to confirm such a tentative assignment.

Summary and Conclusion

When matrices are formed from gas mixtures containing dimethyl ether and argon subjected to electron bombardment matrix isolation conditions, the major products are H_2CO, CH_4, $HCO^{\bullet}$, and CO. The formation of these species is consistent with fragmentation of dimethyl ether cations formed with an internal energy near 5 eV, via charge transfer to Ar^+. The observation of species which are deficient of one hydrogen atom relative to the expected gas-phase products is likely due to hydrogen atom abstraction, as a result of the increased pressures in the reaction zone that are present as a result of matrix isolation conditions. Partial deuteration of dimethyl ether yields results consistent with such H atom/D atom abstractions, providing evidence in support of such a fragmentation pathway.

Acknowledgment. The authors would like to acknowledge the support of the support of NSERC through the Discovery grant program, as well as the work of Ralph Frederick and Ed Wilson for their assistance with equipment maintenance.

References and Notes

(1) Fridgen, T. D.; Zhang, X. K.; Parnis, J. M.; March, R. E. *J. Phys. Chem. A* **2000**, *104*, 3487.
(2) Fridgen, T. D.; Parnis, J. M. *J. Phys. Chem. A* **1997**, *101*, 5117.
(3) Zhang, X.; Parnis, J. M.; Lewars, E. G.; March, R. E. *Can. J. Chem.* **1997**, *75*, 276.
(4) Haney, M. A.; Franklin, J. L. *Trans. Faraday Soc.* **1969**, *65*, 1794.
(5) Botter, R.; Pechine, J. M.; Rosenstock, H. M. *Int. J. Mass Spectrom. Ion Phys.* **1977**, *25*, 7.
(6) Dill, J. D.; Fischer, C. L.; McLafferty, F. W. *J. Am. Chem. Soc.* **1979**, *101*, 6531.
(7) Butler, J.; Holland, D. M.P.; Parr, A. C.; Stockbauer, R. *Int. J. Mass Spectrom. Ion Phys.* **1984**, *58*, 1.
(8) Dutuit, O.; Baer, T.; Metayer, C.; Lemaire, J. *Int. J. Mass Spectrom. Ion Phys.* **1991**, *110*, 67.
(9) Nishimura, T.; Zha, Qingmei, Das, P. R.; Niwa, Y.; Meisels, G. G. *Int. J. Mass Spectrom. Ion Phys.* **1992**, *113*, 177.
(10) Feng, R.; Cooper, G.; Brion, C. E. *Chem. Phys.* **2001**, *270*, 319.
(11) Mejia-Ospino, E.; Garcia, G.; Guerrero, A.; Alvarez, I.; Cisneros, C. *J. Phys. B* **2005**, 109.
(12) Zhu, J.; Guo, W.; Wang, Y.; Wang, L. *Chem. Phys.* **2006**, *326*, 571.
(13) Bouma, W.; Nobes, R. H.; Radom, L. *Org. Mass. Spec.* **1982**, *17*, 315.
(14) Nash, J. J.; Francisco, J. S. *J. Phys. Chem. A* **1998**, *102*, 236.
(15) Peres, R.; Linnert, H. V. *Quim. Nova* **2004**, *27*, 42.
(16) Fridgen, T. D.; Holmes, J. L. *Eur. J. Mass Spectrom.* **2004**, *10*, 747.
(17) Stace, A. J. *J. Am. Chem. Soc.* **1984**, *106*, 4380.
(18) Lassegues, J. C.; Grenie, Y.; Forel, M. T. *Comptes Rend. Seances Acad. Sci. Ser. B* **1970**, *271*, 421.
(19) Khoshkhoo, H.; Nixon, E. B. *Spectromchim. Acta* **1973**, *29A*, 603.
(20) We have previously isolated CO, CH_4 and the other methane isotopomers obtained from commercial sources in argon under matrix isolation conditions in our own laboratory, and observed their wavenumber positions using FTIR spectroscopy.
(21) Moore, B. C.; Pimentel, G. C. *J. Chem. Phys.* **1963**, *38*, 2816.
(22) Milligan, D. E.; Jacox, M. E. *J. Chem. Phys.* **1969**, *51*, 277, and references contained therein.
(23) Fridgen, T. D.; Parnis, J. M. *J. Chem. Phys.* **1998**, *109*, 2155, and references contained therein.
(24) Tso, T-L; Lee, E. K. C. *J. Phys. Chem.* **1984**, *88*, 5475.
(25) Burgers, P. C.; Holmes, J. L. *Org. Mass Spectrom.* **1984**, *19*, 452.
(26) Rosati, R. E.; Skrzypkowski, M. P.; Johnsen, R.; Golde, M. F. *J. Chem. Phys.* **2007**, *126*, 154302.
(27) Baulch, D. L.; Cobos, C. J.; Cox, R. A.; Frank, P.; Hayman, G.; Just, T.; Kerr, J. A.; Murrells, T.; Pilling, M. J.; Troe, J.; Walker, R. W.; Warnatz, J. *J. Phys. Chem.* **1994**, *23*, 847.
(28) Vaskonen, K.; Eloranta, J.; Kiljunen, T.; Kunttu, H. *J. Chem. Phys.* **1999**, *110*, 2122.

JP806689J